International Core Journal of Engineering Volume 11 Issue 3, 2025
ISSN: 2414-1895 DOI: 10.6919/ICJE.202503_11(3).0015

First-principles Study of the Effect of Microstructure on the Corrosion Resistance of CoCrNi Medium Entropy Alloys

Ruili Liu[a]

University of Shanghai for Science and Technology, Shanghai 200082, China

[a]rl18237293839@163.com

Abstract

This paper investigates the effects of ordered and disordered structures on the corrosion resistance of CoCrNi medium-entropy alloys based on first-principle calculations. The adsorption energy results show that O atoms are more favorable to stabilize the FCC sites in the ordered L_{10} structure, indicating that the ordered structure is easier to form a passivation film. O atoms were found to be favored to stabilize at the adsorption sites with more Cr atoms on the surface of both structures CoCrNi(111). In addition, CoCrNi(111)/Cr_2O_3(0001) interfacial binding energy calculations showed a stronger interaction between the ordered L_{10} structure and the metal oxide film. The above results indicate that different alloy structures affect the corrosion resistance of CoCrNi medium-entropy alloys, and the ordered structure has stronger corrosion resistance. The results of this paper can provide theoretical references for the design of corrosion-resistant alloys.

Keywords

First-principle; Medium-entropy Alloys; Passivation Films; Ordered Structures.

1. Introduction

Medium entropy alloy (MEA) is an emerging metallic material, which usually consists of a variety of elements with equimolar or nearly equimolar atomic fractions, and it has a unique microstructure and many excellent properties[1]. Among the many medium-entropy alloys, the FCC CoCrNi MEA has attracted extensive attention from researchers because of its outstanding mechanical properties. Wu et al [2] show that the FCC CoCrNi MEA exhibits the best mechanical properties in the temperature range from -196°C to 400°C. Lu et al [3] show that compared to the CoCrFeMnNi high entropy alloy, CoCrNi MEA has higher strength and excellent fatigue resistance. Yoshida et al [4] comparatively investigated the frictional stress and Hall-Petch relationship between CoCrNi MEA and Ni-40Co alloy, and the results showed that CoCrNi MEA has higher frictional stress.

CoCrNi MEA not only has high mechanical properties, but it also exhibits excellent corrosion resistance and passivation properties. Shang et al [5] showed that the NiCoCr alloy exhibited the best corrosion resistance in both 0.1M NaCl and 0.1M HCl solutions. Feng et al [6] showed that CrCoNi coating in 3.5wt% NaCl solution and 0.5 M H_2SO_4 solution has excellent corrosion resistance and passivation film stability. Zhu et al [7] showed that CoCrNi has superior corrosion resistance than 316L stainless steel, which is mainly related to its passivation film density and stability.

A large number of research on passivation films of CoCrNi MEA has focused on how to improve the corrosion resistance of the alloys by adjusting the composition[8-9]. For example, Wang et al [10] revealed that high Cr content and thicker passivation films resulted in higher corrosion resistance of CoCrNi in acidic solutions. However, studies on the passivation properties of CoCrNi MEA by ordered and disordered structures are rarely reported. In this work, we investigated the effects of

ISSN: 2414-1895 DOI: 10.6919/ICJE.202503_11(3).0015

ordered and disordered structures on the passivation film formation ability of CoCrNi MEA based on first principles calculations to determine the difference in corrosion resistance of CoCrNi MEA with different structures.

2. Theoretical Methods and Calculation Models

All calculations are performed with the Vienna Ab-initio Simulation Package (VASP). The Perdew-Burke-Ernzerhof (PBE) exchange-correlation function under the generalized gradient approximation (GGA) and the projected affixed plane-wave (PAW) pseudopotential were used. The cutoff energy is 450 eV, using a 2 × 2 × 2 Gamma-centered k-point grid. The energy and force convergence criteria were set to 1×10^{-5} eV and 0.02 eV/Å. To avoid the influence of interatomic interactions on the results of the calculations and to reflect the periodicity of the supercell model, a vacuum layer of 15Å is set up in the direction of the z-axis of the model. For the optimization calculations concerning the transition metal oxide Cr_2O_3, the DFT+U method was used for the 3d electrons of Cr, with an effective on-site Coulomb interaction parameter of Ueff = U-J = 3.7 eV.

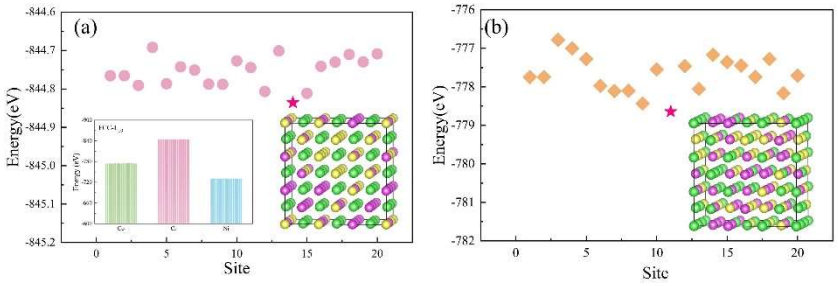

Figure 1. (a) L_{10} CoCrNi MEA, the inset shows the energy comparison of the L_{10} structure when Co, Cr, and Ni are the atoms at the face-centered sites. (b) FCC CoCrNi MEA.

The ordered structure of CoCrNi medium entropy alloy was used FCC-L_{10}, and the disordered structure of CoCrNi was used FCC. The structure was constructed using atomsk. Based on the characteristics of the FCC-L_{10} structure, a structural model was constructed with Co, Cr, and Ni as the atoms in the face-center positions, and the remaining two types of atoms randomly occupying the top corners and the bottom centers in the same proportions, with 20 structures of each type constructed and a total of 60 structures constructed. The energies were calculated and ranked separately, and the structure with the lowest energy was selected for subsequent calculations. The construction of FCC bulk structure model was also randomly constructed with 20 structures, the energies were calculated and ranked separately, and the structure with the lowest energy was selected as the final model. Both structures of CoCrNi MEA are constructed as 3×3×3 supercells containing 108 atoms. The result is shown in Figure 1.

The CoCrNi(111) surface model of FCC, L_{10}, was constructed using atomsk and contains 6 layers of atoms with a total of 108 atoms. The structural model is shown in Figure 2. The L_{10} CoCrNi(111) supercell model was constructed concerning the calculations above. The bottom 4 layers were fixed to simulate the bulk phase and 2 layers of atoms on the surface were released. The adsorption energies were calculated by considering four possible adsorption sites for O atoms on the surface of both structures of CoCrNi(111): the Top site, the Bridge site, the FCC hollow site, and the HCP hollow site. The adsorption energies were calculated by placing O atoms at different adsorption sites on the surfaces of CoCrNi(111) with FCC and L_{10} structures. The adsorption energy was calculated by the following formula.

$$E_{ad} = E_{Slab/O} - E_O - E_{Slab}$$

ISSN: 2414-1895 DOI: 10.6919/ICJE.202503_11(3).0015

where $E_{Slab/O}$ is the total energy of the system with O atoms adsorbed on the surface, E_{clear} is the total energy of the supercell without adsorbed O atoms, and E_O is the energy of the oxygen atom, which is half of the energy of the O_2 molecule used here.

For the interface model construction, the FCC, L_{10} structure of CoCrNi(111) surface are used 1×1×6 supercell structure, which contains a total of 24 atoms. The Cr_2O_3 bulk phase structure model is obtained from the Material Project database, and its (0001) crystalline surface is selected to construct the interface. All models were subjected to structural relaxation to reach a steady state after construction.

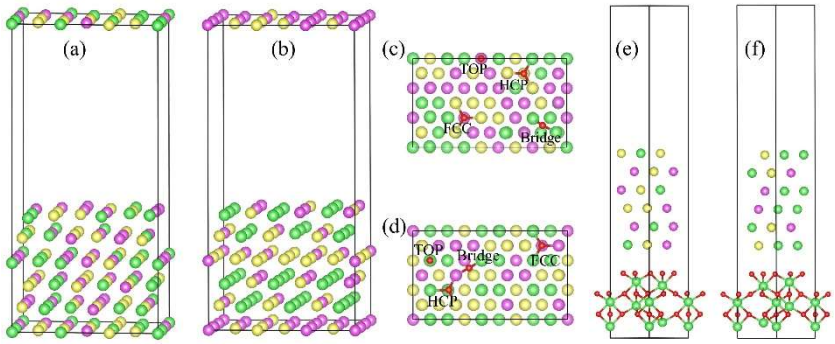

Figure 2. (a) FCC CoCrNi MEA supercell. (b) L_{10} CoCrNi MEA supercell. (c) FCC CoCrNi(111) adsorption sites. (d) L_{10} CoCrNi(111) adsorption sites. (e) FCC CoCrNi(111)/Cr_2O_3(0001) interface structure.(f) L_{10} CoCrNi(111)/ Cr_2O_3 (0001) interface structure.

3. Results and Discussion

3.1 O Adsorption Energy on FCC CoCrNi(111) Surface

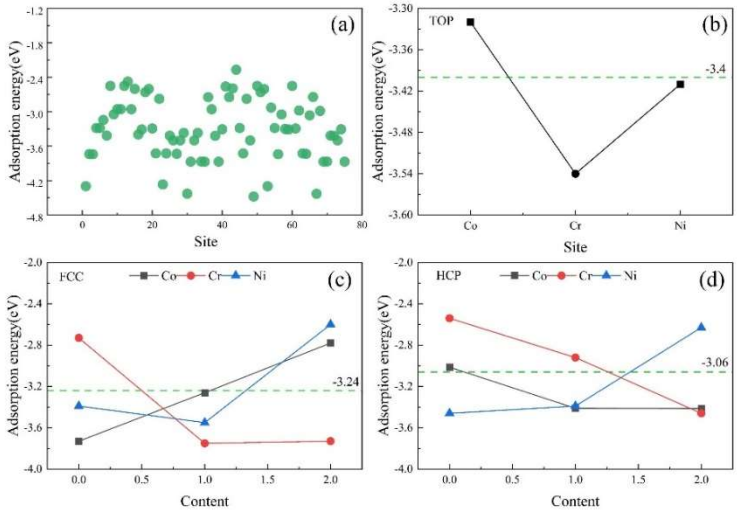

Figure 3. (a) Adsorption energy distribution on the surface of FCC CoCrNi(111). (b) Variation of adsorption energy at TOP sites. (c) O adsorption energies for environments with different contents of metal atoms at the FCC site. (d) O adsorption energies for environments with different contents of metal atoms at HCP sites.

The adsorption of O atoms on the surface of FCC CoCrNi MEA was first analyzed. The calculation results are shown in Figure 3, it is not difficult to find that the adsorption energies of O atoms at all sites on the surface of the FCC structure CoCrNi(111) are negative, indicating that the O atoms can be stabilized in the stabilized adsorption on the surface of the FCC structure CoCrNi(111) supercell. Visualization of the stabilized structure after relaxation reveals that the O atoms initially located at

ISSN: 2414-1895 DOI: 10.6919/ICJE.202503_11(3).0015

the Bridge site, with Co and Ni as terminal TOP sites, migrate to the adjacent FCC and HCP sites after stabilization, while the O atoms at the remaining positions are not shifted. Therefore, O atoms can be stabilized on the surface of FCC CoCrNi(111) supercells adsorbed at FCC, HCP, and TOP sites terminated by Cr atoms. As shown in Figure 3, the variation of adsorption energy is analyzed when the content of metal atoms in different sites is different. Firstly, for the TOP sites, the sites terminated with Cr atoms have the lowest adsorption energy and show the highest stability of O adsorption. In the FCC sites, the O atoms show higher stability at higher Cr atom content. At the HCP sites, the highest adsorption stability is shown at the sites with higher Cr atom content. Thermodynamically, it is shown that the most favorable adsorption site for O atoms on the surface of FCC structural alloys is the TOP site terminated by Cr atoms. Apart from this, the lowest adsorption energy was observed at FCC and HCP sites both with high Cr atom content.

3.2 O Adsorption Energy on L_{10} CoCrNi(111) Surface

The adsorption energies of O atoms at all sites on the surface of L_{10} CoCrNi(111) alloy are negative, indicating that O atoms can be stabilized on the surface of L_{10} CoCrNi MEA. From Figure 4, it is easy to find that the O atom has the lowest average adsorption energy when it is at the FCC site. The same visualization of the adsorption structure after relaxation reveals that the O atoms initially at the Bridge site, as well as Co and Ni as terminal TOP sites, migrate to the adjacent FCC and HCP sites as well and that O can be stably adsorbed in L_{10} alloy at the FCC, HCP, and TOP sites terminated by Cr atoms. The change in the alloy structure did not affect the types of sites where O atoms are favorably adsorbed. The change in adsorption energy of O atoms at the same site type on the alloy surface but in different adsorption atom environments was further analyzed. As shown in Figure 4, at TOP sites, Co and Ni have relatively low adsorption energies when they are terminals, but due to the migration of O atoms from these sites to the neighboring FCC and HCP sites after relaxation. Therefore, the favorable adsorption atomic environments for O atoms at TOP sites are Cr atom terminated. O atoms adsorbed at HCP sites have the lowest adsorption energy in environments with high Cr content. O atoms adsorbed at FCC sites are most favorable for adsorption at sites with high Cr atom content. The overall comparison reveals that O atoms have the lowest average adsorption energy at the FCC site, and in L_{10} CoCrNi MEA, O atoms similarly show a tendency to adsorb at sites with higher Cr atom content.

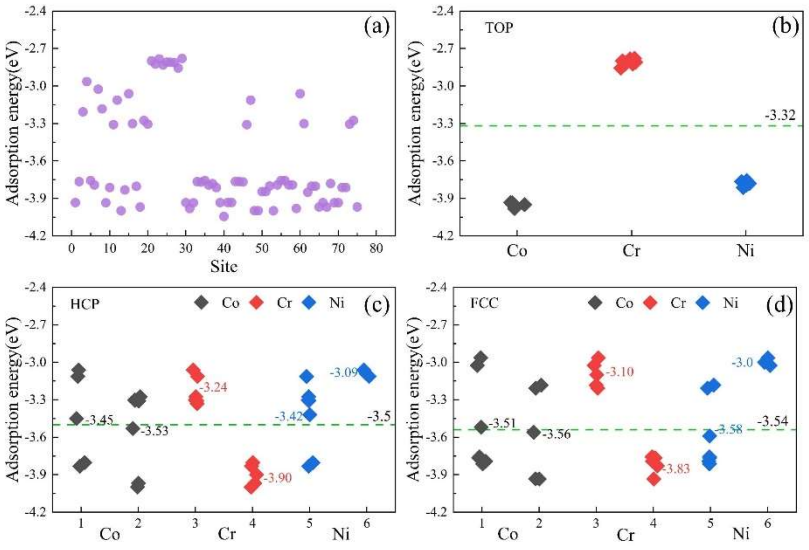

Figure 4. (a) Adsorption energy distribution on the surface of L_{10} CoCrNi(111). (b) Variation of adsorption energy at TOP sites. (c) O adsorption energies for environments with different contents of metal atoms at the HCP site. (d) O adsorption energies for environments with different contents of metal atoms at FCC sites.

ISSN: 2414-1895 DOI: 10.6919/ICJE.202503_11(3).0015

3.3 Comparison of Adsorption Energies of Different Structures

The adsorption stability of O on the metal surface is crucial for the formation of oxide films, and the ease of passivation film formation of different structural alloys was assessed by comparing the adsorption energies indicated by O atoms on the FCC structure and the L_{10} structure CoCrNi MEA. The results are shown in Figure 5, where O atoms exhibit the lowest adsorption energies at the FCC sites on the surface of L_{10} CoCrNi(111). In addition, the average adsorption energy of O atoms on the surface of the L_{10} alloy was lower than that of the FCC alloy. Therefore, O atoms are more favorable to be adsorbed on the surface of L_{10} alloys, and L_{10} CoCrNi MEA are more prone to forming metal oxide passivation films on the surface.

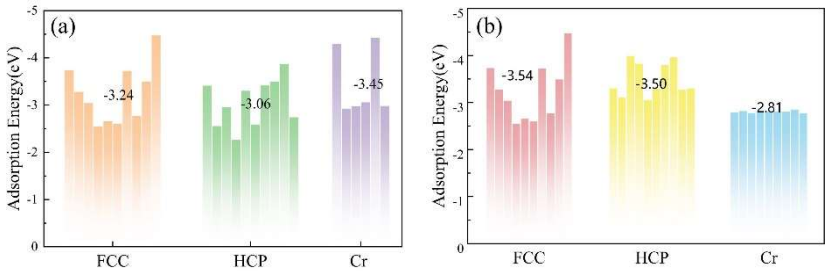

Figure 5. (a) O adsorption energy at CoCrNi(111) surface sites. (a) FCC structure. (b) L_{10} structure.

3.4 CoCrNi(111)/Cr_2O_3(0001) Interface Energy

The main component of the CoCrNi MEA passivation film is an oxide of the metal Cr, Cr_2O_3, which limits the diffusion of O atoms into the alloy and hinders the diffusion of the metal cations outward, thus serving to improve the corrosion resistance of the metal. The corrosion resistance of an alloy and its service life is closely related to the bond strength between the surface oxide film and the base material [11]. To further evaluate the corrosion resistance of different structures of CoCrNi MEA, the interfacial bonding energies of the FCC and L_{10} CoCrNi (111) surfaces and Cr_2O_3(0001) surfaces were calculated. The calculation results are shown in Table 1, the larger the interfacial bonding energy is, the more stable the formed interfacial structure is. Therefore, from the data in the Table 1, it is easy to see that the L_{10} CoCrNi(111)/ Cr_2O_3(0001) interface has greater stability. That is, the bonding ability between CoCrNi MEA with L_{10} structure and passivation film is stronger, indicating that its corrosion resistance is superior.

Table 1. CoCrNi(111)/Cr_2O_3(0001) interface energy.

	E_{total} (eV)	a/b (Å)	Area (Å^2)	$E_{adhesion}$(eV/Å^2)
FCC CoCrNi(111)	-166.64	a=4.98 b=4.98	21.46	
L_{10} CoCrNi(111	-180.97	a=4.98 b=4.96	21.39	
α-Cr_2O_3(0001)	-107.67	a=5.04 b=5.04	21.67	
FCC CoCrNi(111)/Cr_2O_3(0001)	-291.70	a=4.99 b=4.99	21.57	0.81
L_{10} CoCrNi(111)/Cr_2O_3(0001)	-307.05	a=4.99 b=4.98	21.53	0.86

ISSN: 2414-1895 DOI: 10.6919/ICJE.202503_11(3).0015

4. Conclusion

In this study, the effect of ordered and disordered structures on the ability to form passivation films of CoCrNi MEA with equal atomic ratios was investigated. The results show that O atoms are favored to stabilize in FCC, HCP, and TOP sites terminated with Cr atoms in both structured CoCrNi MEA. Among them, the most favorable adsorption site for O atoms in the FCC structural alloy is the TOP site terminated by Cr atoms, and the most favorable adsorption site in the L_{10} structural alloy is the FCC site. The results of interfacial binding energy calculations show that the bonding energy between the ordered structure CoCrNi(111) surface and Cr_2O_3(0001) surface is stronger. The above results indicate that the ordered structure CoCrNi MEA has stronger corrosion resistance compared with the disordered structure. The research results in this paper can provide theoretical guidance for the design of high corrosion-resistant medium entropy alloys.

References

[1] F. He, M. Zhu, Y.F. Yuan, S.Y. Guo, G.T. Zhu, Study on AC Corrosion Behavior of CoCrNi Medium-Entropy Alloy in 3.5% NaCl Solution, Journal of Materials Engineering and Performance (32) (2022) 2918–2931.

[2] Z. Wu, H. Bei, G.M. Pharr, E.P. George, Temperature dependence of the mechanical properties of equiatomic solid solution alloys with face-centered cubic crystal structures, Acta Materialia 81 (2014) 428-441.

[3] K. Lu, A. Chauhan, M. Walter, A.S. Tirunilai, M. Schneider, G. Laplanche, J. Freudenberger, A. Kauffmann, M. Heilmaier, J. Aktaa, Superior low-cycle fatigue properties of CoCrNi compared to CoCrFeMnNi, Scripta Materialia 194 (2021) 113667.

[4] S. Yoshida, T. Bhattacharjee, Y. Bai, N. Tsuji, Friction stress and Hall-Petch relationship in CoCrNi equi-atomic medium entropy alloy processed by severe plastic deformation and subsequent annealing, Scripta Materialia 134 (2017) 33-36.

[5] X. Shang, Z. Wang, F. He, J. Wang, J. Li, J. Yu, The intrinsic mechanism of corrosion resistance for FCC high entropy alloys, Science China Technological Sciences 61(2) (2017) 189-196.

[6] K. Feng, Y. Zhang, Z. Li, C. Yao, L. Yao, C. Fan, Corrosion properties of laser cladded CrCoNi medium entropy alloy coating, Surface and Coatings Technology 397 (2020) 126004.

[7] M. Zhu, F. He, Y. Yuan, S. Guo, G. Wei, A comparative study on the corrosion behavior of CoCrNi medium-entropy alloy and 316L stainless steel in simulated marine environment, Intermetallics 139 (2021) 107370.

[8] S. Zhao, Y. Osetsky, Y. Zhang, Diffusion of point defects in ordered and disordered Ni–Fe alloys, Journal of Alloys and Compounds 805 (2019) 1175-1183.

[9] D. Chakraborty, A. Harms, M.W. Ullah, W.J. Weber, D.S. Aidhy, Effect of atomic order/disorder on vacancy clustering in concentrated NiFe alloys, Computational Materials Science 147 (2018) 194-203.

[10] D.P. Wang, J.W. Shen, Z. Chen, F.G. Chen, P.Y. Guo, Y.X. Geng, Y.X. Wang, Relationship of Corrosion Behavior Between Single-Phase Equiatomic CoCrNi, CoCrNiFe, CoCrNiFeMn Alloys and Their Constituents in NaCl Solution, Acta Metallurgica Sinica (English Letters) 34(11) (2021) 1574-1584.

[11] M.P.J. Punkkinen, K. Kokko, H. Levämäki, M. Ropo, S. Lu, L. Delczeg, H.L. Zhang, E.K. Delczeg-Czirjak, B. Johansson, L. Vitos, Adhesion of the iron–chromium oxide interface from first-principles theory, Journal of Physics: Condensed Matter 25(49) (2013) 495501.